Synthesis and Characterization of Aminolevulinic Acid Gold Nanoparticles: Photo and Sonosensitizer Agent for ....

Article *in* Journal of Luminescence · February 2018

DOI: 10.1016/j.jlumin.2018.01.057

CITATIONS
0

READS
15

3 authors, including:

Daniel Perez Vieira
Instituto de Pesquisas Energéticas e Nucleares
16 PUBLICATIONS **89** CITATIONS
SEE PROFILE

Lilia Courrol
Universidade Federal de São Paulo
174 PUBLICATIONS **1,349** CITATIONS
SEE PROFILE

Journal of Luminescence 197 (2018) 317–323

Contents lists available at ScienceDirect

Journal of Luminescence

journal homepage: www.elsevier.com/locate/jlumin

Synthesis and characterization of aminolevulinic acid gold nanoparticles: Photo and sonosensitizer agent for atherosclerosis

Karina de Oliveira Gonçalves[a], Daniel Perez Vieira[a,b], Lilia Coronato Courrol[a,*]

[a] Instituto de Ciências Ambientais, Químicas e Farmacêuticas, Departamento de Física, Universidade Federal de São Paulo, Rua Arthur Riedel 275, Diadema, São Paulo, Brazil

[b] Centro de Biotecnologia, Instituto de Pesquisas Energéticas e Nucleares, Av. Lineu Prestes 2242, São Paulo, São Paulo, Brazil

ARTICLE INFO

Keywords:
PDT
SDT
Atherosclerosis
ALA
Gold nanoparticles

ABSTRACT

Photodynamic and sonodynamic therapies (PDT and SDT, respectively) are emerging as new atherosclerosis treatments. The subsequent generation of free radicals by activated photo and sonosensitizers can lead to apoptotic cell death. The use of gold nanoparticles (AuNPs) as the vehicle for a sensitizer delivery improves reactive oxygen species formation and sensitizer performance. In this study gold nanoparticles functionalized with polyethylene glycol (PEG) were synthesized mixing δ-aminolevulinic acid (ALA) with tetrachloroauric (III) acid in milliQ water solution followed by photo reduction with 300 W xenon lamp. The synthesized ALA:AuNPs were characterized by UV/vis optical absorption, zeta potential and electron microscopy. The mean particle size of spherical ALA:AuNP was ~ 18 nm, with a polydispersity index of 0.437. Singlet oxygen generation efficiency was measured using the trap molecule 1,3-diphenylisobenzofuran. ALA:AuNPs and DPBF were irradiated with 590 nm LED, or pulse ultrasound irradiation (1 W/cm^2 with 1.0 MHz), and consumption of the DPBF was monitored over time by the absorption and emission spectra. The results showed that he gold nanoparticles generate singlet oxygen during light and ultrasound irradiations. THP-1 cells differentiated into macrophages cytotoxicity test were described and was found the half maximal inhibitory concentration (IC50) values ~ 36 nM for ALA:AuNPs. Increase in the fluorescence intensity of PpIX extracted from macrophages incubated with ALA:AuNPs indicating stable encapsulation of ALA into gold nanoparticles and further conversion to PpIX. The potential use of ALA:AuNps as a sensitizer for photo and sonodynamic therapies were investigated. ALA:AuNPs mediated SDT was more effective than PDT. SDT with ALA:AuNPs induced the reduction of macrophage viability in ~ 87,5% in only 2 min. The mechanism underlying SDT-induced apoptosis involves the generation of singlet oxygen. The results indicate that ALA:AuNPs can be used as a novel photo and sonosensitizer for atherosclerosis.

1. Introduction

Photodynamic therapy (PDT) has been used in the regression of atherosclerotic plaques [1,2]. PDT involves the administration of photosensitizer (PS) molecule that accumulates in the macrophages which are involved in development and thrombogenicity of atherosclerosis. Subsequently the excitation of PS with appropriate wavelength and the presence of molecular oxygen results in reactive oxygen species (ROS) that chemically destroy macrophages [3,4]. However, the application of PDT is limited to superficial lesions. Sonodynamic therapy (SDT) derives from PDT and the main difference between SDT and PDT is the energy source used to activate the sensitizers, in this case ultrasound [5]. However, the significant advantage of SDT over PDT is that ultrasound can penetrate deeply in soft tissue [6].

The principal characteristic of a photo or sonosensitizer must have is ability to preferentially accumulate in macrophages and induce a desired biological effect via the generation of cytotoxic species [7]. Protoporphyrin IX (PpIX) is a key molecule in the diagnosis and treatment of diseases such as atherosclerosis and cancer [8]. This is because tissues affected by these diseases have an accumulation of PpIX [9]. It is known that the external administration of δ-aminolevulinic acid (ALA) causes an accumulation of PpIX in the tissues and this fact has been explored in the photodynamic and sonodynamic therapies [10]. Peng et al. demonstrated that the ALA-derived PpIX can be detected to reflect the macrophage content in the plaque [11] and suggested that ALA mediated PDT could reduce macrophage content and inhibit plaque progression, indicating a promising approach to treat inflamed atherosclerotic plaque. Cheng et al. demonstrated that ALA-SDT exhibited synergistic apoptotic effects on THP-1 macrophages, involving excessive intracellular reactive oxygen species generation and

* Corresponding author.
E-mail address: lccourrol@gmail.com (L.C. Courrol).

https://doi.org/10.1016/j.jlumin.2018.01.057
Received 25 October 2017; Received in revised form 16 January 2018; Accepted 30 January 2018
Available online 01 February 2018
0022-2313/

mitochondrial membrane potential loss [12]. Therefore, ALA-SDT is a potential treatment for atherosclerosis.

The use of gold nanoparticles as carriers of photosensitizers is a very promising approach for PDT and SDT [11]. The association of ALA with gold nanoparticles (AuNPs), increase the applications possibilities of this drug [13–17]. The gold nanoparticles possess a plasmon resonance, a resonant phenomenon where light induces collective oscillations of conductive metal electrons at the NP surface, tunable to different wavelengths by varying the NP size [18]. The AuNPs are very suitable for imaging (MRI, tomography, etc.) and photothermal therapy [19]. The synthesis of nanoparticles are usually carried out by various physical methods like photoreduction [20] and sonification, and chemical methods like co-precipitation [21] and sol-gel technique [22]. Photoreduction synthesis is a clean process which has high spatial resolution, convenience of use, and great versatility [23].

In this study, 5-Aminolevulinic acid (ALA) gold nanoparticles (ALA:AuNPs) functionalized with polyethylene glycol (PEG- were synthetized by photoreduction method and administered to THP-1 macrophage cells to evaluate its toxicity and applications in PDT and SDT.

2. Materials and methods

2.1. ALA:AuNPs solution

The ALA:AuNPs synthesis were performed as previously described [24]. Briefly, 15 mg of $HAuCl_4$ were mixed with 45 mg of ALA and 100 mg of PEG (Poly(ethylene glycol) average mol wt 10,000, Sigma Aldrich) in 100 mL of distilled water at 20 °C. The process was accompanied by vigorous stirring for 5 min, and 10 mL of the resulting solution was exposed to a 300-W xenon lamp for 5 min. The solution pH was adjusted to ~ 7.0.

2.2. ALA:AuNPs characterization

UV–vis absorption spectra were measured by a Shimatzu spectrophotometer, using 1-cm quartz cells.

Shape and sizes of ALA:AuNPs were obtained from a Jeol (Zeiss, Germany) transmission electron microscope. For this, a drop of gold nanoparticles dispersed in distilled water was placed onto a carbon-coated copper grid, the excess liquid was removed using a paper wick, and the deposit was dried in air prior to imaging.

The effective surface charges on the ALA:AuNPs were measured using zeta-potential (Malvern Instruments Zetasizer, Worcestershire, UK).

2.3. Cell culture

Human monocytic leukemia THP-1 cells were cultured in RPMI-1640 medium. Cells were seeded at 5000 cells per well in 96-well plates and incubated at 37 °C in a humidified atmosphere of 5% CO_2 in 95% air. THP-1 cells were treated with 75 nM ng/mL of phorbol myristate acetate (PMA, Sigma-Aldrich Co., St, Louis, MO, USA) for 48 hs to induce differentiation of the cells into macrophages. After differentiation, non-attached cells were removed by aspiration and the adherent macrophages were washed with RPMI-1640 medium 3 times and then incubated in cell culture medium at 37 °C.

2.4. Cell viability assay

PMA pre-stimulated THP-1 cells were incubated with 0–137 nM of ALA:AuNPs for 24 h. Then the cells were washed several times with phosphate buffered saline (PBS) (pH = 7.2–7.6). The ALA-free cells were finally suspended in 500 μL media, and assayed for viability using the colorimetric MTS assay kit based on the CellTiter 96 AQueous One Solution (Promega, Madison, WI, USA), which measures mitochondrial function; the latter correlates with cell viability. In this procedure, the cells were incubated with fresh medium containing MTS reagent for 2 h before measurements at an absorbance of 490 nm. The effect of nanoparticles on cell proliferation was expressed as percentage of inhibition of cell growth relative to the control. Results were statistically compared (ANOVA and Bonferroni post-test) to negative (control cells, NaCl 0.9%) or positive (latex powder suspension, 0.5 g/L - filter sterilized latex extract, 0.5 g/L in culture media, 24 h). The percentage of cell survival was calculated after background absorbance correction and blank absorbance subtraction as follows: % Cell viability = 100 × Experimental well absorbance/untreated control well absorbance.

Table 1
Groups, incubation times and solution concentrations of ALA and ALA: AuNPs. CC (control group).

Groups	Incubation Time (hours)	ALA Concentration nM
(1) ALA:AuNPs	24	68.6
(2) ALA:AuNPs	24	34.3
(3) CC (Cells)	24	–
(4) ALA	4	137.2
(5) ALA:AuNPs	4	68.6
(6) ALA:AuNPs	4	34.3

2.5. PpIX extraction of cells

Around 30.000 cells and 75 ng/mL of PMA were added in each well of a 96 wells plate. After 48 h the macrophages were then divided into groups presented in Table 1.

The contents of each well were collected and added to tubes containing 3 volumes of acetone. These solutions were then centrifuged for 15 min at 4000 rpm, and the supernatants were analyzed in 3 Fluorolog Jobin Yvon fluorimeter. The samples were excited at 400 nm, and emission spectra were measured between 415 and 785 nm. The excitation bandwidth was 5 nm.

2.6. Singlet Oxygen generation

Singlet Oxygen ($^1O_2$) generation was studied from the photodegradation of 1.3-diphenylisobenzofuran (DPBF) [16,17] by absorption and emission spectroscopies. A fresh solution of DPBF (4 μM) in acetone was kept in the dark. For this experiment a 10 mm quartz cuvette containing 1 mL of ALA:AuNPs and 10 μL of DPBF was irradiated with the LED light source at 590 ± 10 nm, InGaN, (VENUS OMEGA-MM OPTICS, Brazil), P~100 mW, by 2 min and removed from the illumination setup to record the absorbance and emission (480 nm with excitation at 422 nm) spectra; this was repeated each 1 min until the sample had been irradiated for 15 min in total.

The singlet oxygen generation induced by irradiation of solutions by ultrasound was studied observing the decrease in the DBPF emission band around 480 nm when solutions were excited at 422 nm. In this case quartz cuvette containing 1.0 mL of ALA:AuNPs and 40 μL of DPBF (4 μM) was irradiated with therapeutic ultrasound HTM Sonic Compact (Brazil). The irradiations were performed with 1 W/cm^2 and 1 MHz frequency. DPBF degradation was evaluated with irradiation from 2 min to 10 min.

2.7. PDT and SDT procedures

The cells followed the protocol described above, and after differentiation into macrophages were incubated with ALA and ALA:AuNPs for 24 h.

For the PDT it was used amber LED at 590 ± 10 nm (VENUS OMEGA-MM OPTICS, Brazil), P~100 mW and exposure time of 2 min.

For the SDT, the transducer of ultrasonic generator, Sonic Compact

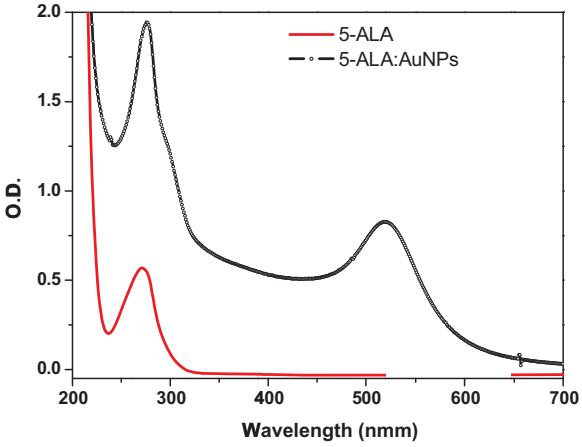

Fig. 1. Absorption spectra of ALA and synthesized ALA:AuNPs (pH~7.0).

from HTM Brazil (diameter 3.5 cm, resonance frequency 1.0 MHz) was placed below the plate containing cells. A fine layer of sterile ultrasound gel was used between transducer and plate. The ultrasonic intensity was 1 W/cm^2. The cells groups were irradiated separately during 2 min. During the sonication procedure, the temperature of the solution increased less than 0.5 °C.

3. Results and discussion

3.1. ALA:AuNPs characterization

The absorbance spectrum of PEGylated ALA:AuNPs solution is shown in Fig. 1. An absorption peak at approximately 522 nm appears due to the SPR (surface plasmon resonance) effect, indicating the formation of gold nanoparticles. The zeta potential of the ALA:AuNPs solutions was measured, in pH ~ 7.0 and the value found was − 23.1 ± 1.0 mV indicating moderate stability solution.

The mean particle size of spherical ALA:AuNP was 18.12 ± 5.94 nm, as shown in the Fig. 2, with a polydispersity index of 0.437.

To estimate the ratio of ALA molecules to Au atoms in the nanoparticles, initially the number of Au atoms in a nanoparticle was calculated considering that the average nanoparticle is spherical, with a 9 nm radius, and that Au crystallizes in a FCC structure with a 407.82 pm side unit cell [25] containing 4 atoms, resulting in ~ 180,000 atoms per nanoparticle. To evaluate the number of ALA molecules attached to the nanoparticle surface, the average nanoparticle surface area (~ 1018 nm^3) was divided by the projected area of the ALA molecule. This area was obtained considering that an ALA molecule is attached to the nanoparticle by its carboxyl group and has an effective radius of 290 pm (estimated using Wolfram Mathematica 11 chemistry database and molecule reconstruction), resulting in a projected area of 0.264 nm^2, and consequently, ~ 3850 ALA molecules attached to the nanoparticle surface. These results provide a ratio of ~ 1/45 ALA molecules per Au atom in a nanoparticle.

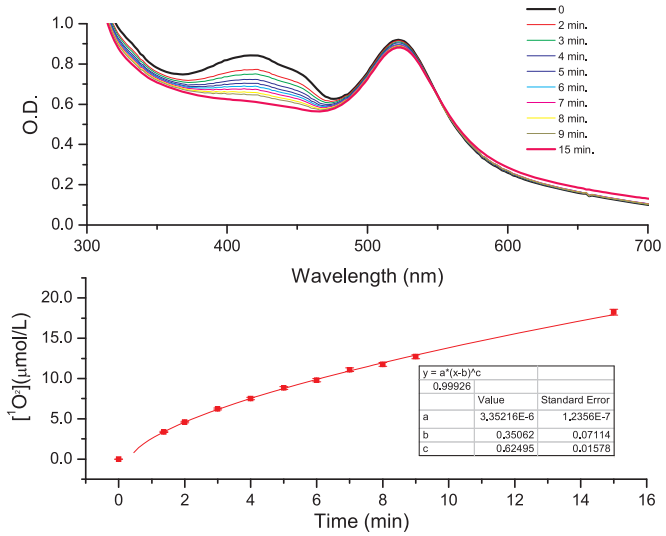

Fig. 3. Gradual DPBF absorbance reduction induced by yellow LED 590 nm irradiation. Singlet oxygen production in function of time.

3.2. Singlet Oxygen generation

1,3-Diphenylisobenzofuran (DPBF), a specific $^1O_2$ trap, dissolved in acetone presents a strong absorption spectrum. A similar spectrum, with a maximum at 422 nm, is obtained when DPBF is incorporated to ALA:AuNPs, shown in Fig. 3a, along it the SPR absorption is also showed at 522 nm. The intensity of DPBF absorption, around 422 nm decreases when DPBF-ALA:AuNPs are exposed to 590 nm irradiation in intervals from 2 to 15 min. The decrease in DPBF absorption intensity occurs due to the reaction between DPBF and $^1O_2$ [26]. Fig. 3a shows the time-dependent decrease in the absorbance at 422 nm via the oxidation of DPBF with ALA:AuNPs.

The amount of $^1O_2$ generated with the irradiation time ($[^1O_2]_t$) can be calculated directly by the consumption of DPBF ($[DPBF]_0$-$[DPBF]_t$)

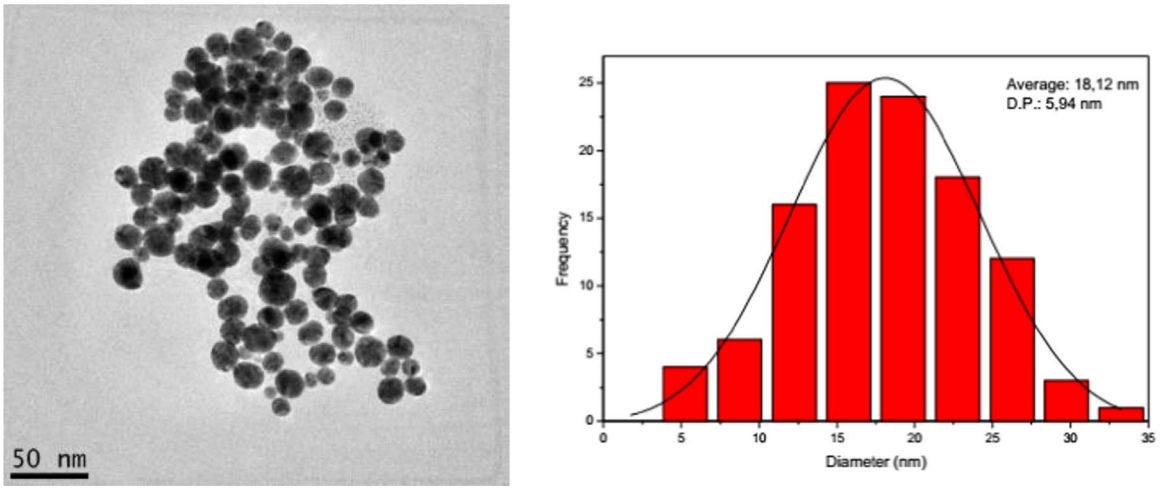

Fig. 2. TEM image and size distribution of synthesized ALA:AuNPs.

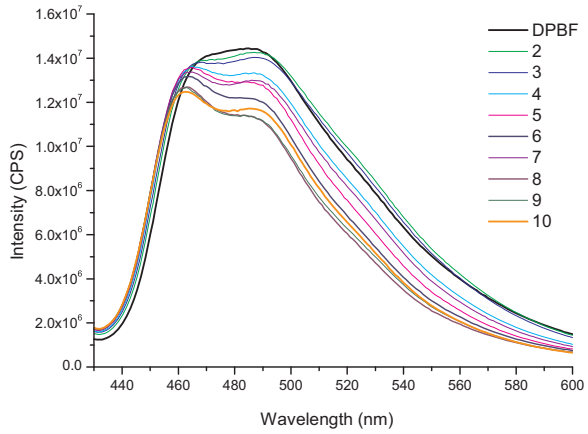

Fig. 4. Fluorescence intensity decreasing of DPBF (4 μM) in ALA:AuNPs solution with the irradiation time of ultrasound irradiation. Excitation, 422 nm.

by the Beer law.

$$[^1O_2]t = [DPBF]_0 - [DPBF]_t = (A_0/\varepsilon_{DPBF}) - (A_t/\varepsilon_{DPBF}) \quad (1)$$

where A_0 and A_t are the absorbance of the mixture in 422 nm at the start and after each time t and ε_{DPBF} = 15,552 L/mol cm. It can be seen in Fig. 3b, irradiation for 15 min generates approximately 20 μmol/L of $^1O_2$. The rate of release of $^1O_2$ under irradiation was ~ 3.7 μmol/(L h).

The production of $^1O_2$ due to ultrasound (US) irradiation was evaluated measuring DPBF fluorescence spectra upon excitation at 422 nm. Fig. 4 shows the decreasing course of DPBF fluorescence with the US irradiation time (in minutes) for ALA:AuNPs.

An obvious enhancement of the singlet oxygen generation from ALA:AuNPs was obtained under 590 nm excitation compared with that of ultrasound as shown in Fig. 5. The experimental points can be fitted by decrease dose-response curves.

3.3. Effects of the ALA:AuNPs on THP-1 Cells

The cytotoxicity effect of ALA:AuNPs in THP-1 cells can be observed in the Fig. 6 where percentage of cell viability is plotted in function of ALA:AuNPs concentration. The percentage of cell viability was calculated as follows: % Cell viability = 100 –% cell cytotoxicity. The % cell cytotoxicity = 100 × (experimental well absorbance –negative control well absorbance)/(positive control well absorbance –negative control well absorbance). All calculations were performed after background absorbance correction and blank absorbance subtraction. From these

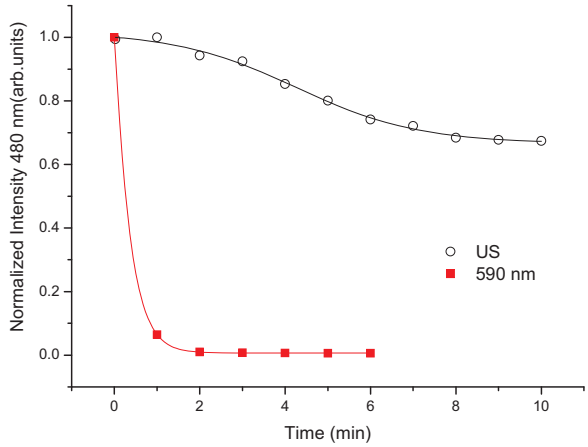

Fig. 5. Time-dependent DPBF fluorescence after irradiation at 590 nm compared with ultrasound (US) 1 MHz and 1 W/cm^2 irradiation. Data obtained comparing 480 nm DPBF fluorescence degradation induced by light and ultrasound, with exciting solutions at 422 nm.

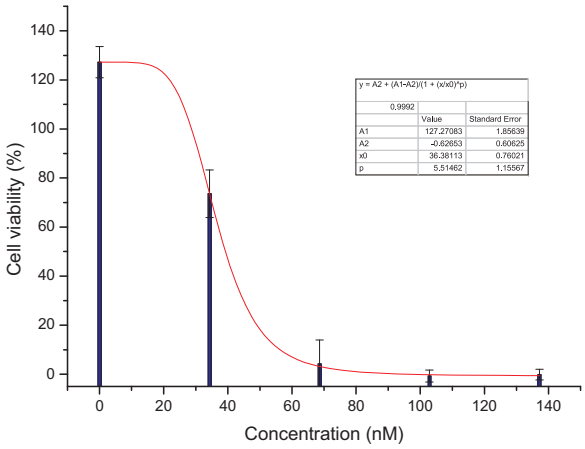

Fig. 6. The cytotoxicity effect of ALA:AuNPs in THP-1 cells. The percentage of cell viability plotted in function of ALA:AuNPs concentration.

results the half maximal inhibitory concentration (IC50) values was found to be ~ 36 nM of ALA:AuNPs.

3.4. Induction of PpIX synthesis

PpIX was extracted with acetone from THP-1 cells exposed to nanoparticles (34 and 69 nM, concentrations) and fluorescence intensities were measured by exciting the samples at 400 nm. The results are presented in Fig. 7. There is an increase in the emission signal around 630 and 700 nm, characteristic of PpIX, with incubation of cells with ALA and ALA:AuNPs for periods of 4 hs (Fig. 7a) and 24 hs (Fig. 7b), when compared to the control group (cells in the culture medium). The results suggest that ALA was incorporated by the gold nanoparticles structure and a quick conversion in endogenous porphyrins occurred, which led to the accumulation of PpIX. After 24 hs incubation with concentrations of 69 nM of ALA:AuNPs, PpIX fluorescence intensity was smaller than for 34 nM. This must be due to reduction in cell viability with ALA:AuNPs at high concentration.

3.5. Cell viability after PDT and SDT treatments

Fig. 8 shows the effects of 2 min of PDT (590 nm) or SDT (1 MHz, 1 W/cm^2) treatments for the control group (CC + PDT/SDT), and cells incubated for 24 h with ALA (134 nM) and ALA:AuNPs (32 nM). The results indicated that although yellow LED and ultrasound did not significantly influence cell viability for the control group, the cell viability with nanoparticles treatment was different after irradiations.

Fig. 8a shows the results of PDT. Cell viability was around 100% in the case of ALA and PDT. The cell viability decreased to ~ 80% in case of ALA:AuNPs and PDT.

Results obtained for SDT are shown in Fig. 8b. The cell viability for ALA and SDT group was ~ 20.1% and for ALA:AuNPs and SDT decreased to ~ 13.5%, showing better inactivation.

4. Discussion

Macrophages appear at a very early stage in the development of atherosclerosis and persist throughout evolution of the disease. Unlike highly proliferating cancer cells, macrophages are specialized phagocytic cells expressing scavenger receptors to help uptake substances as oxidized low-density lipoproteins (oxLDL) and Protoporphyrin IX [27]. The uptake of oxLDL through scavenger receptors of macrophages, transforms macrophages into foam cells. The plaques that form in blood vessels walls are in large part comprised of foam cells. Therefore, a key step in the reduction of plaque formation is the clearance of macrophage cells. Removal of macrophages from atherosclerotic plaques

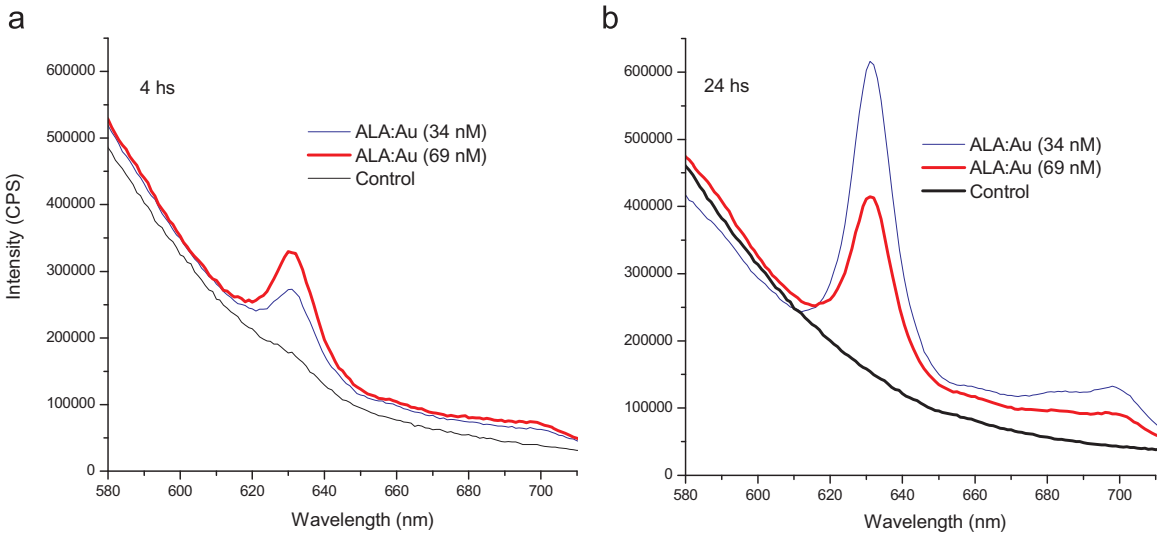

Fig. 7. PPIX fluorescence extracted of cells incubated with ALA:AuNPs (34 and 69 nM, concentrations) for: a) 4 h s and b) 24 h s.

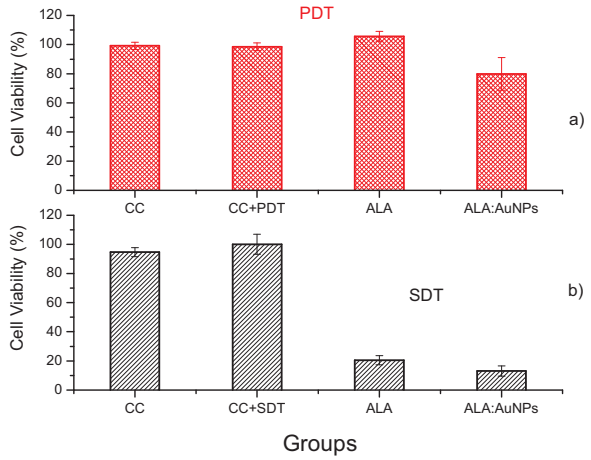

Fig. 8. Viability of THP-1cell after 2 min of a) PDT (LED at 590 nm) and b) SDT (ultrasound with 1 MHz, 1 W/cm^2) treatments for the control group (CC + PDT/SDT), and cells incubated for 24 h with ALA (134 nM) and ALA:AuNPs (32 nM).

could attenuate inflammation and subsequent plaque progression.

Protoporphyrin IX and its derivatives are widely applied in vivo and in vitro to facilitate the macrophage subtraction effects of light and ultrasound [14,15,28–30]. ALA is a natural precursor to sonosensitizer PpIX in the heme biosynthesis pathway. One advantage of exogenous ALA-induced PpIX is that macrophages show a preferential uptake of ALA, increasing synthesis of PpIX [31]. PpIX induces a necrotic cell death in human THP-1 macrophages through activation of reactive oxygen species/c-Jun N-terminal protein kinase pathway and opening of mitochondrial permeability transition pore [32]. Results showed in the Fig. 7, demonstrate an increase in the fluorescence intensity of PpIX by ALA:AuNPs indicating stable encapsulation of ALA into gold nanoparticles and further conversion to fluorescent PpIX. This result indicates that ALA:AuNPs could be used as an atherosclerosis-selective therapeutic agent.

PDT and SDT are promising therapies for macrophages apoptosis [31,33–35]. Previous reports demonstrated PDT and SDT of THP-1 macrophage in vitro with 5-ALA [36,37]. Several studies also demonstrated that ALA in vitro PDT efficiency can be improved by gold nanoparticles [16,38,39]. AuNPs can deliver much more ALA into cells [40]. Furthermore, in a previous publication [41] significantly higher rates of DPBF photobleaching by gold nanoparticles had been reported. As showed by the results presented in the Figs. 3 and 5, the ALA:AuNPs generated singlet oxygen during light irradiation. The photogeneration of $^1O_2$ under CW irradiation is mediated by the initially created "primary hot" electrons; i.e., it occurs during the short time during which the excited electrons have not yet relaxed to a thermal distribution [41]. An alternative possibility for the mechanism of $^1O_2$ photogeneration by gold NPs could be the increased direct photoexcitation of oxygen due to the well-known local electric field enhancement near metal NPs by the plasmon electrons.

The combination of gold nanoparticles-mediated photothermal therapy (PTT) and photosensitizers-mediated PDT was reported by many groups [42,43]. Gold nanospheres have been proven to be useful for photothermal therapy, in which the visible pulsed or CW lasers with wavelength of the peak of surface plasmon resonant absorption were used. For deeper penetration in tissues, near-infrared light must be used. In this study, a LED array at 590 nm was used to induce macrophages cell-killing. This wavelength both photothermal and photodynamic effects can be achieved since can excite gold nanoparticles SPR band and penetrate in the tissue to excite PpIX molecules produced by the cells after ALA:AuNPs incubation.

The results in Fig. 8 indicated the improved macrophage-killing efficiency of ALA:AuNPs in comparison with ALA-PDT. ALA:AuNPs can improve PS uptake [44], enhance PS circulation time and protect PS from deactivation reactions. ALA:AuNPs is converted in PpIX and when PpIX is placed at the vicinity of the AuNPs, the electrons of the PS that are involved in the excitation/emission process, interact with the plasmon field of the metal NP [45]. The interaction results in enhancement of the fluorescence level of PS and consequently of $^1O_2$. So, for ALAAuNPs -based PDT, it is purposed that the efficiency or the cell killing was mainly due to the AuNPs delivery function instead local field enhancement of the AuNPs themselves [40].

According to the results, shown in the Fig. 8, ALAAuNPs mediated SDT was more effective than PDT. The generation of reactive oxygen species from the ultrasonic-activated PpIX were considered to be responsible for the sonodynamic damage of macrophages [12]. In view of the significant depth that ultrasound penetrates in the tissue, SDT provides an advantage over PDT, in which less penetrating light is employed. Acoustic cavitation can activate sensitizers to generate reactive oxygen species (ROS) [46]. Sonoluminescence, a process whereby light is generated upon irradiation of a solution with the ultrasound, is believed as another key mechanism to generate ROS.

5. Conclusion

The method of synthesis of nanoparticles with 5- ALA is considered

green, since it does not use toxic reducers; is quite reproducible, simple and compatible for therapeutic applications. The characterizations of nanoparticles have shown that they have good stability and homogeneous distribution. PEG acts as a stabilizer, and makes the biocompatible nanoparticles. From cytotoxicity effect of ALA:AuNPs on THP-1 cells assay test it was found the half maximal inhibitory concentration (IC50) values ~ 36 nM for ALA:AuNPs. PpIX fluorescence measurements demonstrated that 5-ALA was incorporated by the gold nanoparticles and a quick conversion in endogenous porphyrins occurred, which led to the accumulation of PpIX. We demonstrated that SDT with ALA:AuNPs induced the reduction of macrophage viability in ~ 87,5% in only 2 min. One of the mechanism underlying SDT-induced apoptosis involves the generation of singlet oxygen. The results indicate that ALA:AuNPs are promising sonosensitizer agents for atherosclerosis.

Acknowledgements

This work was supported by the “Fundação de Amparo a Pesquisa do Estado de São Paulo” (FAPESP), Grant no. 2010/016544-1.

References

[1] J.W.H. Wennink, Y. Liu, P.I. Makinen, F. Setaro, A. de la Escosura, M. Bourajjaj, J.P. Lappalainen, L.P. Holappa, J.B. van den Dikkenberg, M. al Fartousi, P.N. Trohopoulos, S. Yla-Herttuala, T. Torres, W.E. Hennink, C.F. van Nostrum, Macrophage selective photodynamic therapy by meta-tetra(hydroxyphenyl) chlorin loaded polymeric micelles: a possible treatment for cardiovascular diseases, Eur. J. Pharm. Sci. 107 (2017) 112–125.

[2] R. Waksman, P.E. McEwan, T.I. Moore, R. Pakala, F.D. Kolodgie, D.G. Hellinga, R.C. Seabron, S.J. Rychnovsky, J. Vasek, R.W. Scott, R. Virmani, PhotoPoint photodynamic therapy promotes stabilization of atherosclerotic plaques and inhibits plaque progression, J. Am. Coll. Cardiol. 52 (12) (2008) 1024–1032.

[3] R. Virmani, A.P. Burke, A. Farb, F.D. Kolodgie, Pathology of the vulnerable plaque, J. Am. Coll. Cardiol. 47 (8) (2006) C13–C18.

[4] C.J. Schwartz, A.J. Valente, E.A. Sprague, J.L. Kelley, R.M. Nerem, The pathogenesis OF atherosclerosis - an overview, Clin. Cardiol. 14 (2) (1991) 1–16.

[5] A.K.W. Wood, C.M. Sehgal, A review of low-intensity ultrasound for cancer therapy, Ultrasound Med. Biol. 41 (4) (2015) 905–928.

[6] M. Trendowski, The promise of sonodynamic therapy, Cancer Metastas. Rev. 33 (1) (2014) 143–160.

[7] H.G. Jeong, M.S. Choi, Design and properties of porphyrin-based singlet oxygen generator, Isr. J. Chem. 56 (2–3) (2016) 110–118.

[8] M. Nascimento da Silva, L.B. Sicchieri, F. Rodrigues de Oliveira Silva, M.F. Andrade, L.C. Courrol, Liquid biopsy of atherosclerosis using protoporphyrin IX as a biomarker, Analyst 139 (6) (2014) 1383–1388.

[9] F.R. de Oliveira Silva, M. Helena Bellini, V. Regina Tristao, N. Schor, N.D. Vieira Jr., L.C. Courrol, Intrinsic fluorescence of protoporphyrin IX from blood samples can yield information on the growth of prostate tumours, J. Fluoresc. 20 (6) (2010) 1159–1165.

[10] F.R. de Oliveira Silva, M.H. Bellini, C.T. Nabeshima, N. Schor, N.D. Vieira Jr., L.C. Courrol, Enhancement of blood porphyrin emission intensity with aminolevulinic acid administration: a new concept for photodynamic diagnosis of early prostate cancer, Photodiagn. Photodyn. Ther. 8 (1) (2011) 7–13.

[11] C.H. Peng, Y.S. Li, H.J. Liang, J.L. Cheng, Q.S. Li, X. Sun, Z.T. Li, F.P. Wang, Y.Y. Guo, Z. Tian, L.M. Yang, Y. Tian, Z.G. Zhang, W.W. Cao, Detection and photodynamic therapy of inflamed atherosclerotic plaques in the carotid artery of rabbits, J. Photochem. Photobiol. B-Biol. 102 (1) (2011) 26–31.

[12] J.L. Cheng, X. Sun, S.Y. Guo, W. Cao, H.B. Chen, Y.H. Jin, B. Li, Q.N. Li, H. Wang, Z. Wang, Q. Zhou, P. Wang, Z.G. Zhang, W.W. Cao, Y. Tian, Effects of 5-aminolevulinic acid-mediated sonodynamic therapy on macrophages, Int. J. Nanomed. 8 (2013) 669–676.

[13] M.K.K. Oo, X. Yang, H. Du, H. Wang, 5-aminolevulinic acid-conjugated gold nanoparticles for photodynamic therapy of cancer, Nanomedicine 3 (6) (2008) 777–786.

[14] J.N. Wu, Y. Lin, H. Li, Q. Jin, J. Ji, Zwitterionic stealth peptide-capped 5-aminolevulinic acid prodrug nanoparticles for targeted photodynamic therapy, J. Colloid Interface Sci. 485 (2017) 251–259.

[15] J.N. Wu, H.J. Han, Q. Jin, Z.H. Li, H. Li, J. Ji, Design and proof of programmed 5-aminolevulinic acid prodrug nanocarriers for targeted photodynamic cancer therapy, ACS Appl. Mater. Interfaces 9 (17) (2017) 14596–14605.

[16] Kd.O. Goncalves, M.N. da Silva, L.B. Sicchieri, F.R. de Oliveira Silva, R.A. de Matos, L.C. Courrol, Aminolevulinic acid with gold nanoparticles: a novel theranostic agent for atherosclerosis, Analyst 140 (6) (2015) 1974–1980.

[17] M. Benito, V. Martin, M.D. Blanco, J.M. Teijon, C. Gomez, Cooperative effect of 5-aminolevulinic acid and gold nanoparticles for photodynamic therapy of cancer, J. Pharm. Sci. 102 (8) (2013) 2760–2769.

[18] V. Voliani, Update on Gold Nanoparticles from Cathedral Windows to Nanomedicine, EBSCO Ebook Academic Collection, ISmithers Rapra Pub., Shrewsbury, 2013, p. 1 (online resource) (vi, 148 pages).

[19] C. Louis, O. Pluchery, Gold nanoparticles for physics, chemistry and biology, Imperial College Press; Distributed by World Scientific Pub. Co., London; Singapore, 2012.

[20] P. Kshirsagar, S.S. Sangaru, M.A. Malvindi, L. Martiradonna, R. Cingolani, P.P. Pompa, Synthesis of highly stable silver nanoparticles by photoreduction and their size fractionation by phase transfer method, Colloids Surf. A-Physicochem. Eng. Asp. 392 (1) (2011) 264–270.

[21] I. Shlar, E. Poverenov, Y. Vinokur, B. Horev, S. Droby, V. Rodov, High-throughput screening of nanoparticle-stabilizing ligands: application to preparing antimicrobial curcumin nanoparticles by antisolvent precipitation, Nano-Micro Lett. 7 (1) (2015) 68–79.

[22] R. Gupta, A. Kumar, Bioactive materials for biomedical applications using sol-gel technology, Biomed. Mater. 3 (3) (2008).

[23] X.F. Zhang, Z.G. Liu, W. Shen, S. Gurunathan, Silver nanoparticles: synthesis, characterization, properties, applications, and therapeutic approaches, Int. J. Mol. Sci. 17 (9) (2016) 34.

[24] O.G. Karina, N.S. Monica, B.S. Leticia, C.C. Lilia, Green synthesis of gold nanoparticles with aminolevulinic acid of: a novel theranostic agent for atherosclerosis, BBA Clin. 3 (S) (2015) S13.

[25] Wolfram Research, Wolfram Alpha, 2018. ⟨http://www.wolframalpha.com/input/?I=gold+LatticeConstant.2018⟩.

[26] K.D. Belfield, M.V. Bondar, O.V. Przhonska, Singlet oxygen quantum yield determination for a fluorene-based two-photon photosensitizer, J. Fluoresc. 16 (1) (2006) 111–117.

[27] Q. Liu, M.R. Hamblin, Macrophage-targeted photodynamic therapy: scavenger receptor expression and activation state, Int. J. Immunopathol. Pharmacol. 18 (3) (2005) 391–402.

[28] Y. Shimamura, D. Tamatani, S. Kuniyasu, Y. Mizuki, T. Suzuki, H. Katsura, H. Yamada, Y. Endo, T. Osaki, M. Ishizuka, T. Tanaka, N. Yamanaka, T. Kurahashi, Y. Uto, 5-Aminolevulinic acid enhances ultrasound-mediated antitumor activity via mitochondrial oxidative damage in breast cancer, Anticancer Res. 36 (7) (2016) 3607–3612.

[29] X. Yang, P. Palasuberniam, D. Kraus, B. Chen, Aminolevulinic acid-based tumor detection and therapy: molecular mechanisms and strategies for enhancement, Int. J. Mol. Sci. 16 (10) (2015) 25865–25880.

[30] T. Feuerstein, G. Berkovitch-Luria, A. Nudelman, A. Rephaeli, Z. Malik, Modulating ALA-PDT efficacy of mutlidrug resistant MCF-7 breast cancer cells using ALA prodrug, Photochem. Photobiol. Sci. 10 (12) (2011) 1926–1933.

[31] S.Y. Guo, X. Sun, J.L. Cheng, H.B. Xu, J.H. Dan, J. Shen, Q. Zhou, Y. Zhang, L.L. Meng, W.W. Cao, Y. Tian, Apoptosis of THP-1 macrophages induced by protoporphyrin IX-mediated sonodynamic therapy, Int. J. Nanomed. 8 (2013) 2239–2246.

[32] H.B. Xu, Y. Sun, Y. Zhang, W. Wang, J.H. Dan, J.T. Yao, H.B. Chen, F. Tian, X. Sun, S.Y. Guo, Z. Tian, Y. Tian, Protoporphyrin IX induces a necrotic cell death in human THP-1 macrophages through activation of reactive oxygen species/c-Jun N-terminal protein kinase pathway and opening of mitochondrial permeability transition pore, Cell. Physiol. Biochem. 34 (6) (2014) 1835–1848.

[33] L.B. Zheng, X.Y. Sun, X. Zhu, F.X. Lv, Z.Y. Zhong, F. Zhang, W.H. Guo, W.W. Cao, L.M. Yang, Y. Tian, Apoptosis of THP-1 derived macrophages induced by sonodynamic therapy using a new sonosensitizer hydroxyl acetylated curcumin, PLoS One 9 (3) (2014).

[34] H. Wang, X. Zhu, R.L. Han, X. Wang, L.M. Yang, Y. Wang, Near-infrared light activated photodynamic therapy of THP-1 macrophages based on core-shell structured upconversion nanoparticles, Microporous Mesoporous Mater. 239 (2017) 78–85.

[35] Z.T. Li, X. Sun, S.Y. Guo, L.P. Wang, T.Y. Wang, C.H. Peng, W. Wang, Z. Tian, R.B. Zhao, W.W. Cao, Y. Tian, Rapid stabilisation of atherosclerotic plaque with 5-aminolevulinic acid-mediated sonodynamic therapy, Thromb. Haemost. 114 (4) (2015) 793–803.

[36] F. Tian, J.T. Yao, M. Yan, X. Sun, W. Wang, W.W. Gao, Z. Tian, S.Y. Guo, Z.X. Dong, B.C. Li, T.L. Gao, P. Shan, B. Liu, H.Y. Wang, J.L. Cheng, Q.P. Gao, Z.G. Zhang, W.W. Cao, Y. Tian, 5-Aminolevulinic acid-mediated sonodynamic therapy inhibits RIPK1/RIPK3-dependent necroptosis in THP-1-derived foam cells, Sci. Rep. 6 (2016).

[37] J.E. Mateus, W. Valdivieso, I.P. Hernandez, F. Martinez, E. Paez, P. Escobar, Cell accumulation and antileishmanial effect of exogenous and endogenous protoporphyrin IX after photodynamic treatment, Biomedica 34 (4) (2014) 589–597.

[38] M.K.K. Oo, X. Yang, H. Wang, H. Du, 5-aminolevulinic Acid Conjugated Gold Nanoparticles for Cancer Treatment, 2008.

[39] S.M. Amini, S. Kharrazi, M. Hadizadeh, M. Fateh, R. Saber, Effect of gold nanoparticles on photodynamic efficiency of 5-aminolevolenic acid photosensitiser in epidermal carcinoma cell line: an in vitro study, IET Nanobiotechnol. 7 (4) (2013) 151–156.

[40] Z.X. Zhang, S.J. Wang, H. Xu, B. Wang, C.P. Yao, Role of 5-aminolevulinic acid-conjugated gold nanoparticles for photodynamic therapy of cancer, J. Biomed. Opt. 20 (5) (2015) 8.

[41] S.J. Chadwick, D. Salah, P.M. Livesey, M. Brust, M. Volk, Singlet oxygen generation by laser irradiation of gold nanoparticles, J. Phys. Chem. C 120 (19) (2016) 10647–10657.

[42] C.P. Yao, L.W. Zhang, J. Wang, Y.L. He, J. Xin, S.J. Wang, H. Xu, Z.X. Zhang, Gold nanoparticle mediated phototherapy for cancer, J. Nanomater. (2016).

[43] J.M. Bergen, H.A. Von Recum, T.T. Goodman, A.P. Massey, S.H. Pun, Gold nanoparticles as a versatile platform for optimizing physicochemical parameters for targeted drug delivery, Macromol. Biosci. 6 (7) (2006) 506–516.

[44] Z. Zhang, Y.S. Chen, J.Y. Ding, C.L. Zhang, A. Zhang, D.N. He, Y.X. Zhang, Biocompatible 5-aminolevulinic acid/Au nanoparticle-loaded ethosomal vesicles

for in vitro transdermal synergistic photodynamic/photothermal therapy of hypertrophic scars, Nanoscale Res. Lett. 12 (2017).
[45] E. Dulkeith, A.C. Morteani, T. Niedereichholz, T.A. Klar, J. Feldmann, S.A. Levi, F. van Veggel, D.N. Reinhoudt, M. Moller, D.I. Gittins, Fluorescence quenching of dye molecules near gold nanoparticles: radiative and nonradiative effects, Phys. Rev. Lett. 89 (20) (2002).
[46] S. Umemura, K. Kawabata, K. Sasaki, N. Yumita, K. Umemura, R. Nishigaki, Recent advances in sonodynamic approach to cancer therapy, Ultrason. Sonochem. 3 (3) (1996) S187–S191.